The Development of Hopping Capabilities for Small Robots

Paolo Fiorini
Department of Informatics
University of Verona
Verona, Italy 37134

Joel Burdick
Mechanical Engineering
California Institute of Technology
Pasadena, California 91125

Abstract: *This paper describes the development of small hopping robots that are suitable for many tasks in unknown, rugged terrain. We describe the evolution of our hopping robot concept by way of the main prototypes that we have developed. These prototypes show that a small robot can move effectively by hopping provided that it is equipped with steering, jumping, and self-righting capabilities. The last prototype is equipped with wheels to achieve precision motion after landing. Lessons learned during the development of these prototypes have general applicability to the design of hopping robots. In addition to reviewing some of the key aspects of the design of jumping systems, this paper gives detailed pictures and descriptions of the mechanism of the various prototypes.*

1 Introduction and Motivation

This paper describes the addition of *hopping* capabilities to small robots. This development is motivated by the need of utilizing small autonomous robots, equipped with excellent mobility to overcome large obstacles, for a variety of applications, ranging from space missions to Mars and other celestial bodies to Earth exploration, surveillance and search and rescue operations. Space missions are usually characterized by a low to medium gravitational environment and share with Earth applications the need of traversing unstructured terrain. The space exploration community has significant interest in the development of new mechanical mobility systems in support of exploration missions, whereas military , intelligence and disaster prevention communities look for new devices to improve their operational capabilities.

The development presented in this paper represents the evolution of the proof-of-concept of a mobility concept that can be useful for implementing alternative design paradigms that employ light weight vehicles, as represented by the three prototypes shown in Fig. 1. To understand the motivation for our approach, we first briefly review the main mobility paradigms for exploration robots, their advantages and some of their drawbacks.

To date, the most successful autonomous exploration robot is the 6-wheeled rover Sojourner, of the Mars Pathfinder mission [14]. Because of its unique rocker-bogey suspension, a 6-wheeled rover of the Sojourner type can traverse obstacles that are about 1.5 times the vehicle's wheel diameter. However, this still represents only a fraction of the vehicle's overall body length. Moreover, this design relies upon a significant number of actuators and complex suspension linkages. For example, the Sojourner mobility system used 10 motors, while prototypes for planned Mars missions use 12 independent actuators [21]. Inflatable wheels may be able to overcome somewhat proportionally larger obstacles. Nonetheless, wheeled designs have fundamental limitations on the obstacle size, compared to body length, that can be overcome. Thus, some terrains are not accessible to wheeled

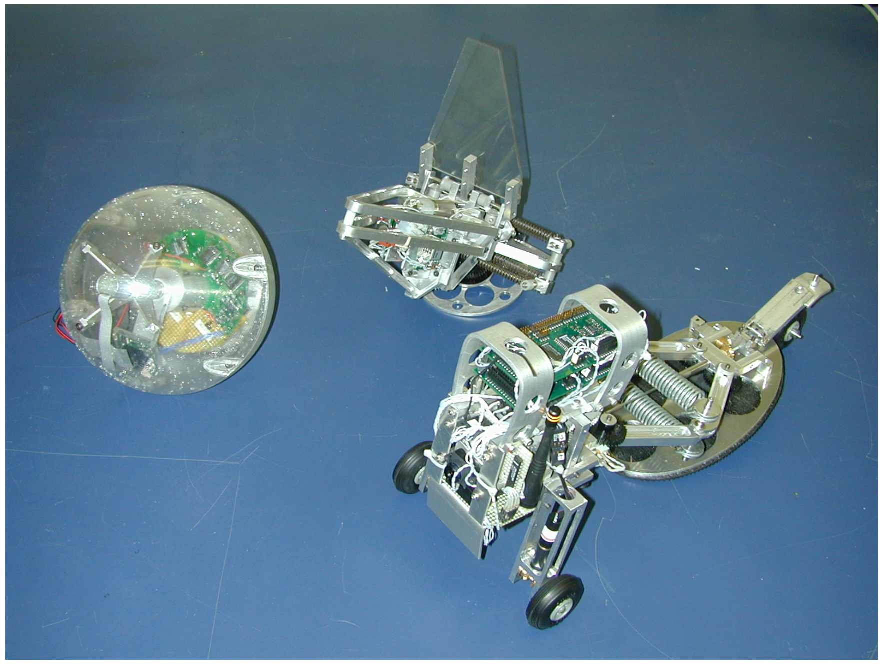

Figure 1: The three generations of hopping robots described in the paper.

vehicles. Terrain accessibility may become a problem as vehicles are scaled down in size in order to enable multi-vehicle design approaches. Researchers at the Jet Propulsion Laboratory have successfully demonstrated small (1 kg mass) 4-wheeled exploratory rovers in realistic simulated conditions [22]. However, because of the fundamental limitations imposed by wheels, these vehicles can only go over obstacles a few cm in height.

Legged robots can overcome the limited traversability of wheeled vehicles in many rugged terrains. Legged rovers have previously been proposed for Lunar and Martian exploration [1], and large legged vehicles have been demonstrated in the tough environment of an Alaskan volcano [2]. While legged robots can potentially access rough terrains, they are mechanically complex, requiring numerous joints, actuators, and linkages. While spiders and insects can demonstrate impressive ability to climb over obstacles, it is not yet clear that multi-legged robot vehicles have impressive ability to overcome large obstacles when the are scaled down in size.

As discussed above, even wheeled rover vehicles use a significant numbers of actuators and complex suspension linkages. Hence, most paradigms for small exploration robots are based on a large number of actuators and complex suspension linkages, with the obvious risks associated to using many motors and linkages.

In this work we describe the development of a different paradigm based on jumping across obstacles to overcome their relatively small dimension, provided that they can reliably survive the landing impact. The discussion in Sections 2 shows that hopping can be a realistic alternative to wheels in many rugged environments. Our hoppers' operation, which is described below, is similar to the movement of a frog, rather than the oscillatory behavior of well known hopping robots [16].

In summary, our goal is to develop small jumping devices. However, a truly small device may not have the functionality necessary to carry out meaningful tasks. The development described in this paper explores the trade-offs between functionality and complexity in the context of the design and development of simple hopping robots. As an example of the benefits of our approach, our second generation hopping design demonstrates that a single actuator is enough to propel, steer, and self-right a simple hopper. The same actuator can also pan an on-board camera. Furthermore, the entire system weighs less than 1.3 Kg, and efficiently converts stored energy to hopping motion.

This system has demonstrated leaps of 12-15 body lengths. Hence, a single actuation design offers surprising capability, compactness, and efficiency.

The paper is organized as follows. Section 2 summarizes the relevant prior work in this area. Section 3 describes the first prototype, and summarizes its performance and some of its shortcomings. Next Section 4 describes the second generation system *the frogbot*, and some of our laboratory experiments. The third generation prototype, the *Wheeled hopper*, is described in Section 5, which tries to overcome some of the mobility limitations of the second generation. Finally, Section 6 summarizes the main aspects of our research and presents our plans for future research in this area.

2 Past Work

Hopping systems for planetary mobility were first proposed in Ref.s [15, 18] as a promising transportation concept for astronauts in a Lunar environment. A first order analysis of Lunar hopper performance is presented in Ref. [10]. The authors propose a single-seat device propelled by a gas actuated leg hinged under the astronaut seat and stabilized by four elastic legs. The acceleration intensity and duration is limited by the tolerance of the human body. Automatic reorientation of the hopper is not supported in this design concept. A two-seat hopping laboratory which is capable of changing direction during the stance phase is also briefly discussed. Based on data from the Apollo missions, the paper also compares different approaches to Lunar transportation, showing that hopping can be an efficient form of transportation in a low-gravity environment, as shown in Table 1. The Table shows in matrix form three mobility systems and fours performance parameters: traveled distance (Distance), total weight (Weight), useful load (Payload) and Autonomy. None of these conceptual studies was reduced to practice.

Mobility	Distance (km)	Weight (kg)	Payload (kg)	Autonomy
Hopper	30	450	7	3 hours
Rocket	7	205	7	131 Kg of propellant
Rover	17	1750	larger	Several hours

Table 1: Comparison Lunar mobility systems.

More recently, a hopping robot, whose structure is the precursor for some aspects of our first generation device, is described in [13]. Motion discontinuity is common to all of the systems described in this paper, since a pause for reorientation and recharge of the thrust mechanism is inserted between jumps.

Laboratory demonstrations of hopping robots have generally focused on continuous motion and dynamic stability, without pauses between jumps. Raibert's seminal work in this area is summarized in [16], and analyzed mathematically in several works, such as Ref.s [11, 12, 17].

Research on non-holonomic systems has motivated a renewed interest in the control of hopping robots. An often analyzed device is the "Acrobot", a reversed double-pendulum with a single actuator located in the joint and free to move its base [3, 7, 9, 20]. Ref. [3] describes how to make the Acrobot jump by accelerating its center of mass until the base loses ground contact. Since the acrobot uses only one actuator, it is only capable of motion on the vertical plane. In contrast, our single motor 2^{nd} generation hopper is not restricted in its motions.

The closest relevant work to ours comes from the impressive "scout" robot development program at the University of Minnesota [6]. The scout is a small two wheeled vehicle containing a leaf spring whose deployment can cause the scout to leap a small distance for purposes of jumping up one stair or overcoming obstacles. The scout was designed for operation in indoor environments, and therefore its two wheels and low ground clearance are mainly suited for movement on smooth floors. In contract, we are targeting outdoor environments.

In the last few years, smaller wheeled rovers for planetary exploration have been designed and fabricated in several research laboratories. The interest in these systems is motivated by the fact that they can be effectively used in many tasks, from planetary exploration to search and rescue operations. The *Nanorover* developed at the NASA Jet Propulsion Laboratory [22] consists of a body (with approximate dimensions of 15 cm x 15 cm x 5 cm) equipped with four movable struts each carrying a 6 cm wheel equipped with an internal motor and with helical cleats for skid steering.

An earlier prototype of the first generation rover described in Section 3 is presented in more detail in Ref. [8]. We briefly summarize this system because some of the computing, electrical, and sensing subsystems are the same in both generations, and thus need only be discussed once.

3 The First Generation Design

Fig. 2 shows the internal components of the first generation design. A clear polycarbonate shell surrounds the mechanism, and is attached to the body at the upper support and lower plate, as is shown in Fig. 3 and Fig. 4. The shell protects the mechanism during crash landings. Its transparency allows the internal camera to collect images. Control of the vehicle by a single actuator is implemented with the aide of an over-running clutch. With the decoupling action of the clutch, rotation of the motor in one direction drives the leg compression and leg release subsystem, while rotation in the other direction drives the camera rotation.

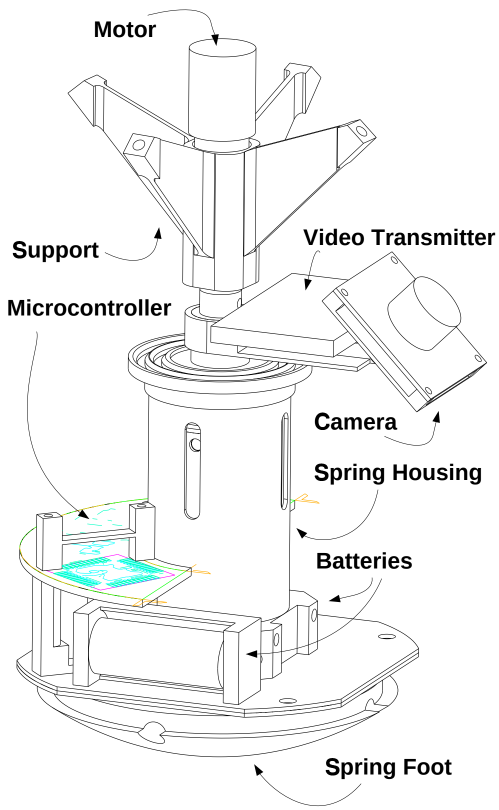

Figure 2: Schematic drawing of the 1^{st} generation mechanism. The surrounding polycarbonate shell is omitted for clarity.

Figure 3: Photograph of the 1^{st} generation system.

Vertical hopping motions are generated by the release of a simple linear spring, which is compressed after each jump via a ball screw that is driven by the motor. The spring housing consists of two concentric cylinders that guide the spring's compression/decompression. The compressed spring is held in place by a spring-loaded ball bearing lock-release mechanism [8]. This mechanism locks after a fixed amount of spring compression is reached. A few extra motor rotations beyond the locking point causes the mechanism to release. By reversing the motor rotation, a camera can be rotated so as to take images through the clear shell. The body's orientation can also be modified by rotating the camera, whose off-axis center of mass causes the vehicle to tilt. Steering (the act of pointing the vehicle in the desired direction before take-off) is achieved via this concept by tilting the vehicle in the desired direction prior to launch. Since the camera is an off-center mass, the tilting is achieved by pointing the camera in the desired hopping direction. The self-righting capability is implemented passively in this design by creating a low center of mass, locating the batteries and heavy components in the bottom of the hopper. The hopper takes off, flies, and lands with the bottom downward.

The electronic subsystem consists of a microcontroller board that contains a PIC CMOS microprocessor, motor controller and power circuits, communication ports, and analog/digital signal acquisition. The board consumes $\sim$ .35 Watts, excluding motor and science instruments. Additionally, the major board components have power-down features to conserve energy. Power is provided by four 12 V batteries. The video micro-camera broadcasts images on channel 14 by an RF transmitter.

A number of tests were performed to assess this first design. We first focus on its jumping ability, and then summarize other useful observations. Even after experimental optimization of the thrust spring, this prototype only realized vertical jumping heights of about 80 cm and horizontal leaping distances of 30-60 cm. We determined that most of energy that was stored in the spring was not converted to motion during the launching process.

Our experiments showed that the hopper achieved only a 20% efficiency. I.e., 80% of the energy

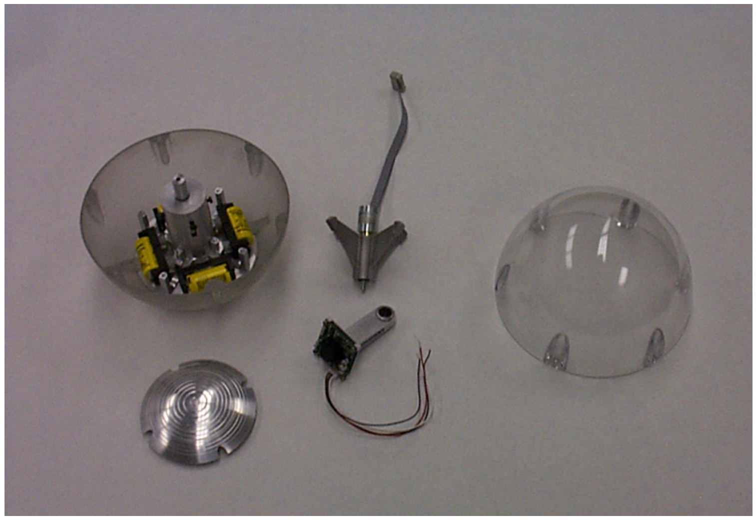

Figure 4: Internal components of the 1^{st} generation system.

stored in the spring was not converted into hopper motion. Instead, this energy is dissipated by friction and wasted motions of the mass-spring thrusting system. A large number of factors, such as internal dissipation of the spring material as well as friction in the moving and locking mechanisms, each contributed to this dissipation. However, three factors dominated the losses. First, at the end of decompression phase, the foot abruptly stops in an elastic impact with a mechanical stop, thereby dissipating its kinetic energy. The magnitude of this loss is proportional to the ratio of foot' mass to total mass. In this design, the loss equals 15% of the spring's stored energy. Clearly, one should always reduce the foot's mass to minimize this loss in this design, and all designs where the motion of an extending is checked by a mechanical stop. Because the hopper tilts in order to steer, the ground reaction force is often not normal to the surface, and may fall outside the Coulomb friction cone. In this case, slippage and energy loss occurs during take-off. Should the hopper prematurely leave the ground before the spring is fully extended, part of the spring's stored energy will not be usefully converted to kinetic energy. In fact, premature lift-off is particularly bad for linear springs, where more of the useful work is realized near the end of the decompression cycle. Such premature lift-off was observed in some of our experiments.

Besides inefficiency, the first generation design had other drawbacks. First, the passive self-righting system will clearly not work in many terrains, and is therefore not robust. I.e., if the vehicle landed on hard ground, and subsequently tumbled onto a sandy spot, it may become irretrievably stuck on its side in the soft sand. Second, the steering system was not reliable. Again, in soft ground, the rotation of the off-axis camera did not reliably cause the body to tilt in the desired direction.

4 The Second Generation Design

The goal of the second generation design was to solve the three major shortcomings of the first generation system: (1) inefficient hopping; (2) unrobust steering; (3) unrobust self-righting capability. To overcome these shortcomings of the first generation design, this generation uses an active steering mechanism, an active self-righting system, and a novel energy storage/thrusting system. Each of these subsystems is described below.

Figure 5 shows the vehicle in its compressed state. In its compressed state, the robot fits into a

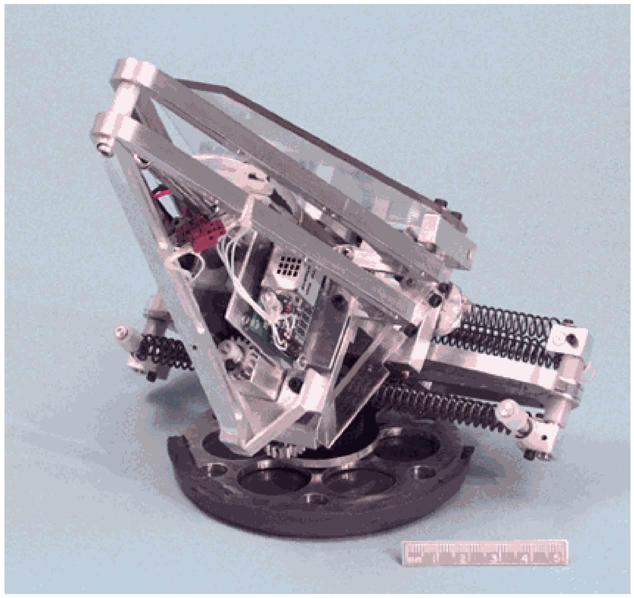

Figure 5: Photo of 2^{nd} Generation hopper in compressed state . The ruler in the photograph has a total length of 5 cm.

roughly $15 \times 15 \times 15$ cm^3 space. Its total weight, including battery pack, is approximately 1.3 kg.

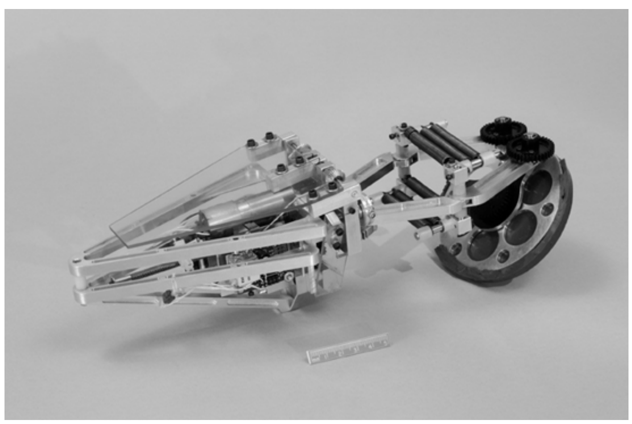

Figure 6: Photo of 2^{nd} Generation hopper in uncompressed state. The ruler in the photograph has a total length of 5 cm. The battery is not shown.

Figure 6 shows a photograph of the second generation system in its uncompressed state.

To solve the problems of inefficiency and high holding force, we turned to a combined spring/linkage mechanism. Fig. 7 depicts the geometry of a geared 6-bar spring/linkage system that we have found to be surprisingly effective. Fig. 8 shows a photograph of its mechanical implementation in both its compressed and uncompressed states. The leg extension is along the y-direction in Fig. 7. Displacements in the y-direction induce, through the linkage, displacements in the linear spring along the x-direction. In effect, the linkage creates a nonlinear spring from a linear spring. In addition, this concept can be practically implemented in a stiff structure with low internal friction.

The surprising utility of this linkage can be understood by noticing that the maximum leg thrust is realized in the middle of the thrusting phase, while the thrust force at the onset of lift-off is quite low. This force/displacement profile substantially reduces the likelihood of premature lift-off due to the shocks inherent in initial spring release. Additionally, when this leg is nearly fully compressed,

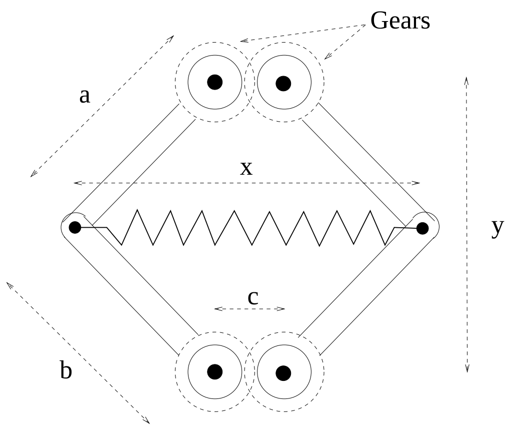

Figure 7: (a) Schematic diagram of the 2^{nd} generation energy storage linkage, a 6-bar geared mechanism.

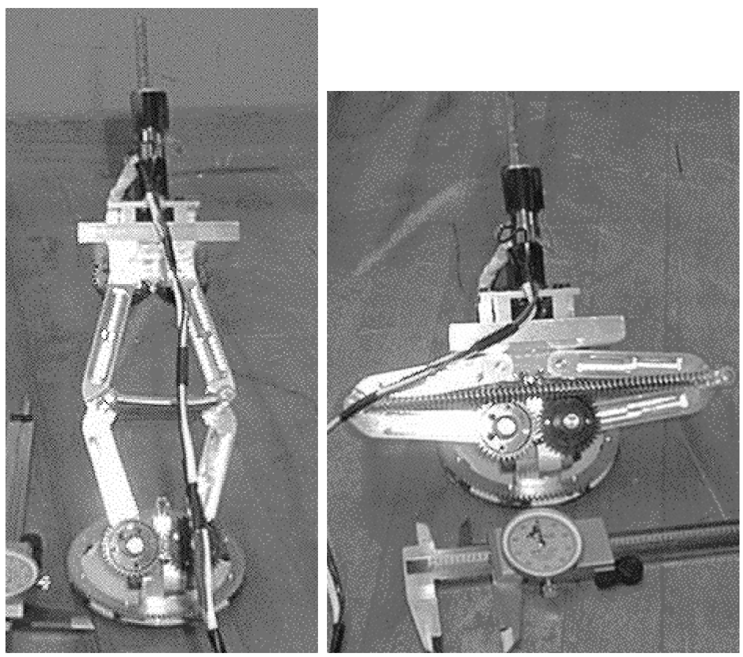

Figure 8: (a) Photo of 2^{nd} generation thrust leg: (a) uncompressed; (b) compressed state. The self-righting mechanisms and crash cage are removed for clarity.

very little force is required to maintain the compressed state. Hence, after energy is stored in the leg, a surprising small amount of force is required to maintain the leg in its compressed state.

Mechanically, the primary motor compresses the leg via a power screw. The screw is driven until it connects with a latching mechanism, whereupon leg compression commences. The leg is compressed until a micro-switch is tripped. When the robot is ready to hop, a small amount of additional compression causes a mating wedge on the 6-bar to release the leg latch. The entire assembly is mounted at a roughly 50 degree angle with respect to the foot's horizontal axis. This fixed take-off angle roughly optimizes the horizontal hopping distance over a wide variety of ground characteristics.

Experiments with this system showed that this leg design realizes a 70% mechanical energy conversion efficiency, versus 20% for the first generation linear spring design. As shown in the experiments below, this high efficiency enables long hops.

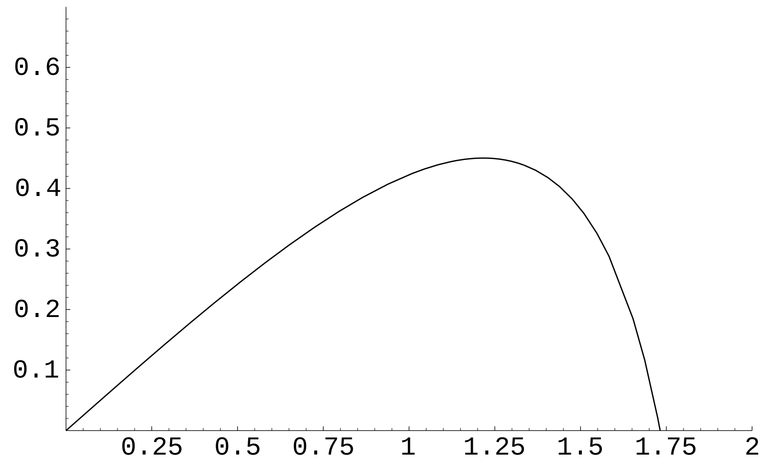

Figure 9: Reaction Force vs. leg extension for the 6-bar geared linkage (case $a = b$, and normalized spring constant).

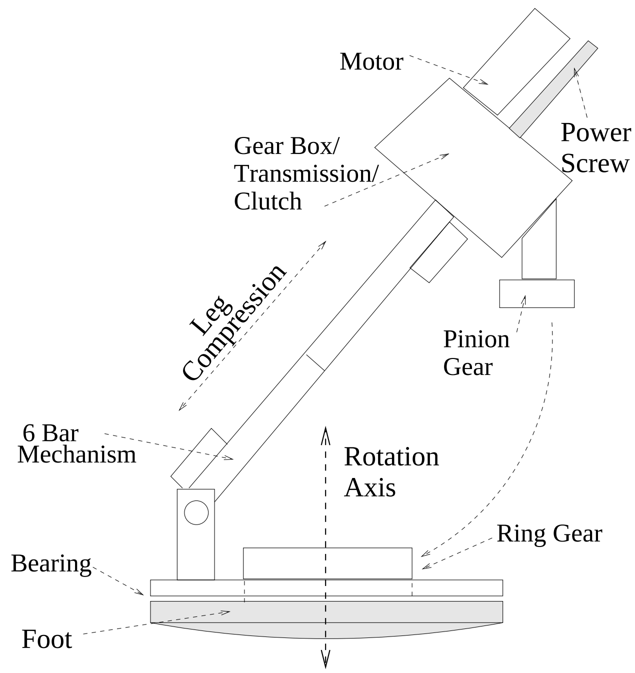

Figure 10: Schematic of steering mechanism. The self-righting mechanism, crash cage, and several components are omitted for clarity.

To robustly and accurately point this system in a desired direction, as well as to point the on-board camera, the second generation device employs an active steering mechanism. The main robot structure is attached to the foot by a bearing that rotates about the vertical axis (Fig. 10). When the leg reaches its maximum compression, a pinion gear that is driven by the primary motor engages with a ring gear that is rigidly attached to the foot. Rotation of the pinion controls the steering angle. Since the camera is attached to the upper body, steering can also implement panning of an on-board camera. Note that steering is unidirectional.

The hopper will typically land in an unpredictable toppled configuration. To cope with a large variety of possible landing configurations, a two stage self-righting process and self-righting mechanism was designed. The outer profile of the hopper's crash cage is roughly a triangular prism. Hence, after a hop, the uncompressed system is very likely to come to rest on one of the prism's

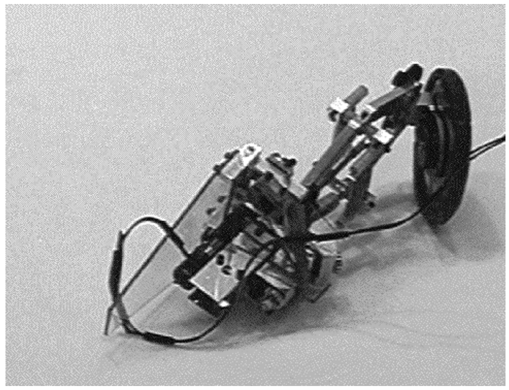

Figure 11: Landing configuration.

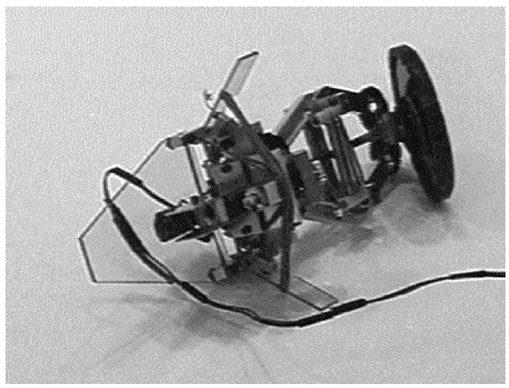

Figure 12: First phase of self-righting sequence. Side flaps are opening.

faces. During the *first phase* of the self-righting process, flaps (whose stored configurations make up part of two faces) open up, causing the hopper to roll onto its back face. In the *second phase*, the rotation of a large flap (that is initially flush with the hopper's back face) forces the hopper toward an upright configuration. The leg compression phase is timed to coincide with this part of the self-righting process, and moves the hopper's center of mass to aid the uprighting process. The leg is compressed by the end of phase II, preparing the vehicle for subsequent hops. With this two phase process, the hopper can nearly always be brought to an upright position, in preparation for the next operational cycle. The hopper's broad foot combined with its low center of mass in the compressed state ensures that the upright posture is statically stable. Fig.s 11 through 15 show digitized images from a video that captures a complete cycle of the hopper's operation. The cycle begins with the robot in a posture like that of Fig. 5. After steering to the intended direction, the leg is released.

The main hopper subsystems were outlined above. A key novelty of our design is its ability to drive all of these subsystems with a single motor. Like the first generation design, we use an overrunning clutch to allow opposite motor rotations to drive different operations. However, the second generation design cycles through more operations, and novel timing mechanisms, mechanical logic, and couplers were introduced to coordinate the various actions.

We tested this device on a variety of surfaces. It typically jumps a horizontal distance of 2.3 – 3 m, and reaches a vertical height of $\sim$ 1.2 m during free-flight. This system could potentially overcome physical obstacles of considerable size. Fig. 16 shows a blurry image of the device during free-flight.

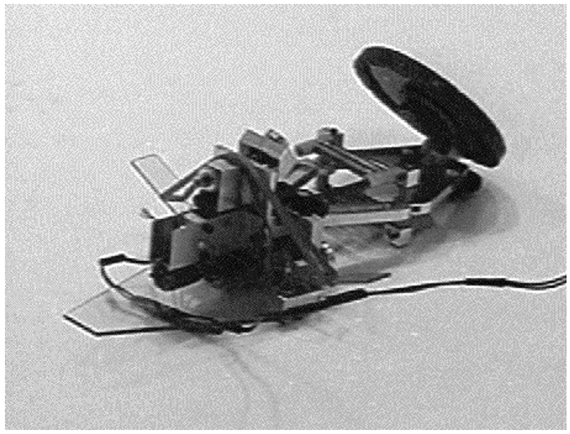

Figure 13: Posture at end of self-righting phase I.

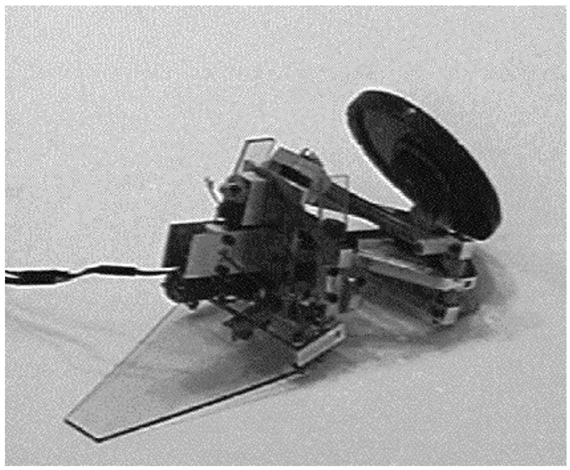

Figure 14: Second phase of self-righting sequence.

5 Generation Three: The Wheeled Hopper

The "generation two" hopper had two main shortcomings:

1. *The lack of an adjustable take-off angle.* An adjustable take-off would enable the robot to better pinpoint its landings and to tailor its aerial trajectories for specific obstacles.

2. *The lack of fine mobility.* The lack of wheels, treads, or other means to implement fine adjustment of the robot's position on the terrain limits its maneuverability.

The 3^{rd} generation device contained components that addressed these shortcomings. It retained the 6-bar thrusting mechanism, while adding two driven wheels and a mechanism to adjust the take-off angle. This system also incorporated realistic on-board computation and wireless communication.

Figure 17 shows the Hopper in the take off position. In this picture, the main visible component of the hopper is the gear-box to compress the thrusting springs. In the second generation, the spring was compressed by a rigid power screw. In this prototype, the spring is compressed by winding a cable on a capstan. The cable's retraction compresses the spring.

The third wheel at the rear of the hopper is a passive caster for stability. This wheel is attached to the output of a 4-bar mechanism, whose motion is driven by the take-off angle adjustment system. In the compressed configuration, the robot must be able to drive around. To enable this,

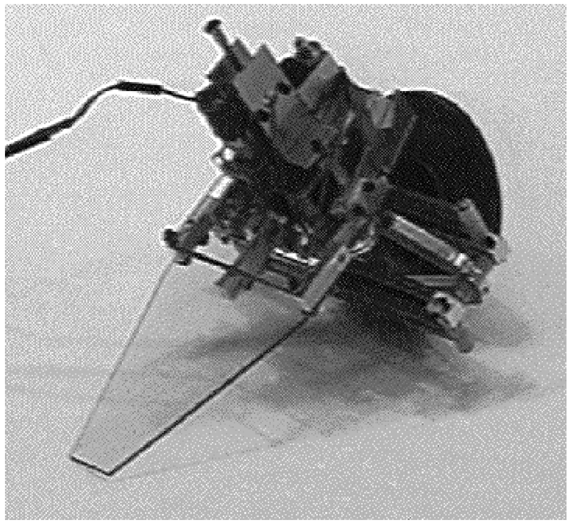

Figure 15: Second phase of self-righting sequence.

Figure 16: Flight Phase.

the foot is tucked up under the vehicle, while the rear wheel is lowered to a functional position. In preparation for launch, the foot is lowered while the rear wheel is simultaneously raised by the coupled action of the 4-bar. Once the foot contacts the ground, continued movement of the angle adjustment system increases the take-off angle. In this prototype, the take-off angle could be continuously adjusted from 0^o to $\sim 85^o$, as showin in Fig 18. Figure 19 shows the extended linkage attached to the rear of the gear-box, and the cable used to compress the leg.

The wheels shown in photographs are clearly not intended for use in rough terrain. Instead, they allow conceptual and functional tests. The hopper's foot is elliptical to support different take-off positions. Fine motion control is provided by the two front wheels, which can steer the robot to the desired hopping direction. The hopper drives while its leg is in the compressed configuration.

In order to realistically assess the practical impact of a full on-board electronics suite the component packing geometry and overall system mass, this prototype is equipped with an electronic package, surrounding the gear-box, providing motor control, programmability, and communication with a remote operator. Power is provided by four primary 12 V batteries. The instrument suite is currently simulated by a video micro-camera, mounted in front of the hopper, broadcasting images directly to operator's PC. The crash cage added to the hopper to protect the electronics during crash landing, is clearly visible in Figure 20.

The complete system, including the operator station is shown in Figure 21. The operator station consists of a lap top computer equipped with two radio links: a full duplex channel for command and data exchange with the hopper, and a TV link to download images taken by the on-board camera. The computer screen shown in Figure 21 displays a window of the hopper camera imaging the computer mouse, and the command windows. Using icons in the command window, the operator can control the hopper motion, initiate a hop, and acquire data about wheel position and take off angle.

Figure 22 shows one experiment to verify the operational capabilities of the hopper in a simulated terrain. During this first capability test, the hopper was able to drive on a flat carpeted area and easily hopped over rocks approximately 30 cm high, all under remote operator control.

6 Conclusion

This paper describes a novel jumping paradigm which can potentially enable small vehicles to overcome significant obstacles in unstructured terrain. The second generation hopper offered surprising capability and reasonable efficiency in a small package that contains a single actuator. We verified in our third generation that a small jumping system can also deploy wheels for fine mobility, control its jumping take-off angle, while also containing sufficient onboard computing and communication capability to carry out realistic tasks.

There are clearly several avenues of future work. Our second generation design achieved significant hopping distances, good efficiency, and robust steering. While it's self-righting ability has been successful in our trials, we currently have no proof that the vehicle can self-right itself in all possible terrains with all possible contact conditions. From the practical point of view, the use of more exotic structural materials (such as carbon-fiber composites) and exotic energy storage schemes should reduce the size and weight of future prototypes. Finally, the jumping/hopping paradigm

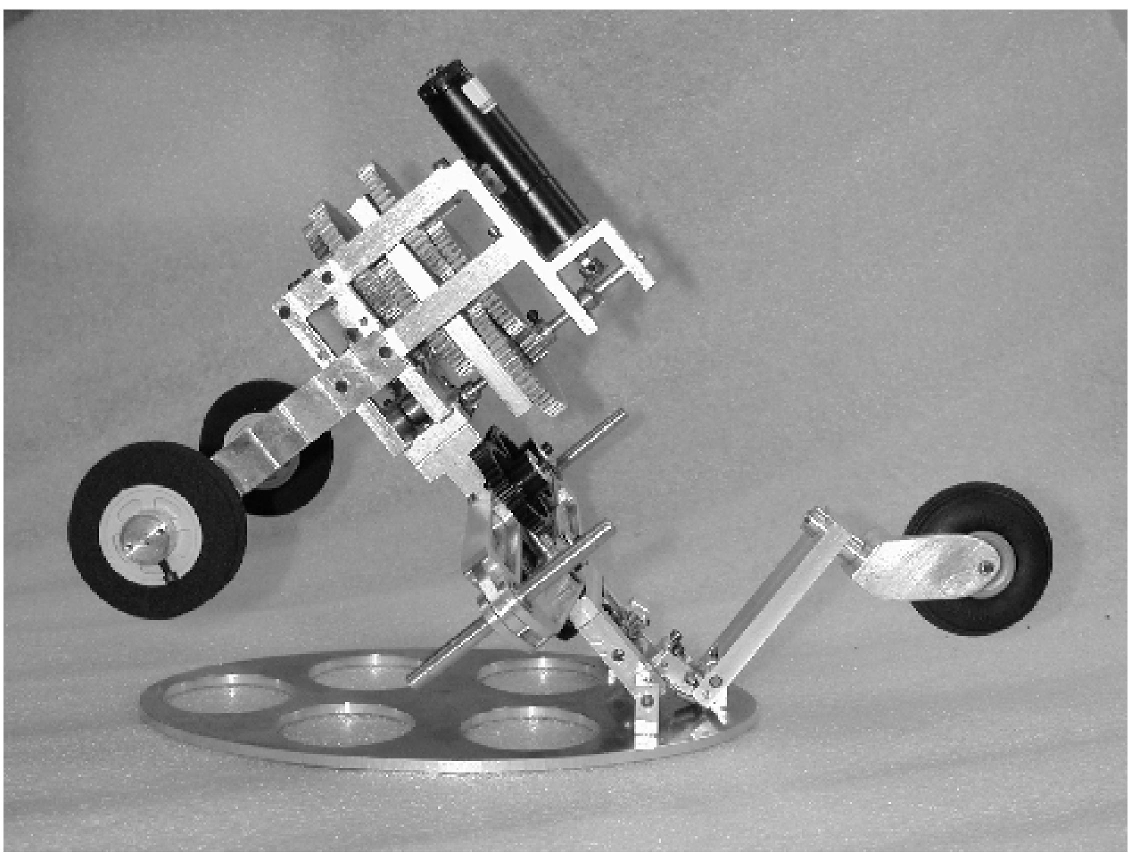

Figure 17: The Hopper 3^{rd} in take-off position.

poses several challenging issues in the development of navigation and localization algorithms.

Acknowledgments: This work was supported by the Jet Propulsion Laboratory, California Institute of Technology (Caltech), under contract with the National Aeronautics and Space Administration. This work was also partially funded by a grant from the National Science Foundation through the Center for Neuromorphic Systems Engineering at Caltech, grant NSF9402726. The authors thank Andy Tretten, Matt Heverly, Jeff Gensler, Eric Hale, Nathan Schara, Steve Schell, Ed Barlow and Sawyer B. Fuller for their design and fabrication support, and Samad Hayati and Neville Marzwell of JPL-NASA for their financial support and encouragement.

References

[1] J. Bares, M. Hebert, T. Kanade, E. Krotkov, T. Mitchell, R. Simmons, and W. Whittaker. Ambler: An autonomous rover for planetary exploration. *IEEE Computer*, 22(6):18–26, Aug. 1989.

[2] J. Bares and D. Wettergreen. Dante ii: Technical description, results, and lessons learned. *Int. J. of Robotics Research*, 18(7):621–649, July 1999.

[3] M.D. Berkemeier and R.S. Fearing. Sliding and hopping gaits for the underactuated acrobot. *IEEE Tran. on Robotics and Automation*, 14(4):629–634, 1998.

[4] S. Bhattacharya and S.K. Agrawal. Spherical rolling robot: A design and motion planning study. *IEEE Trans. on Robotics and Automation*, 16(6):835–839, Dec. 2000.

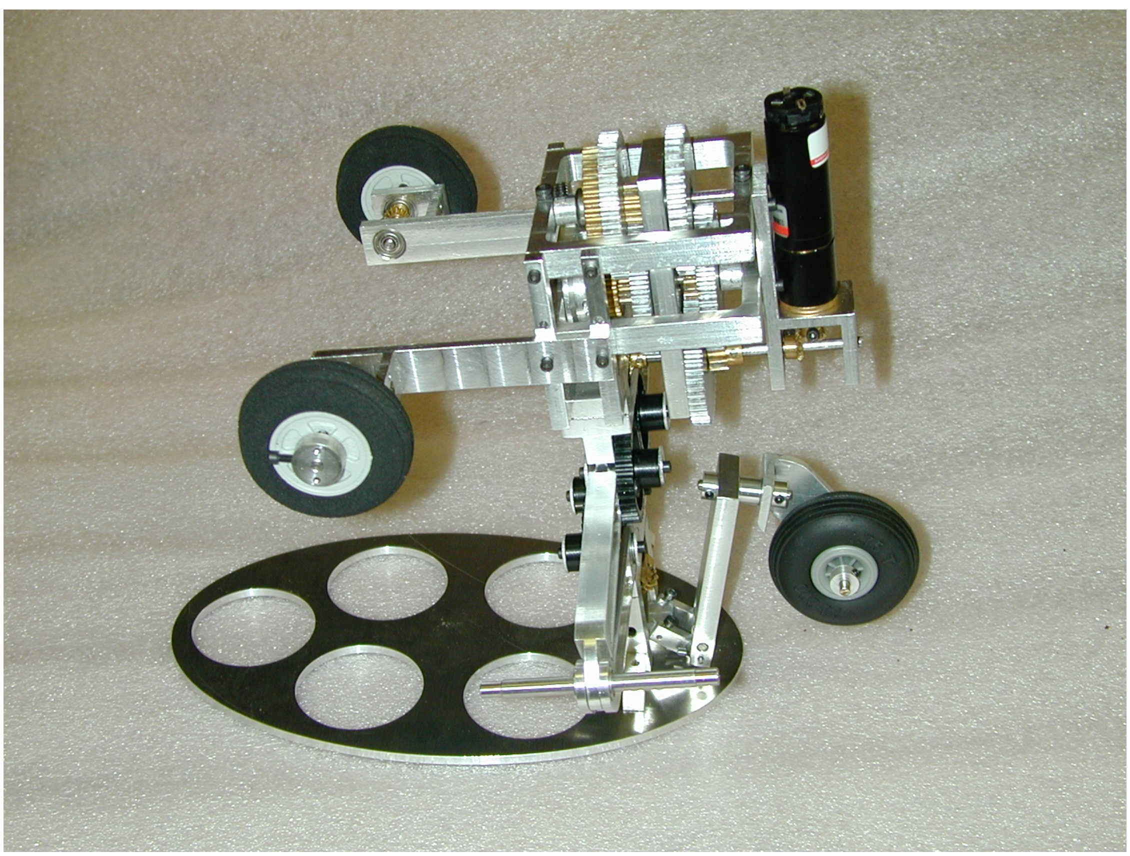

Figure 18: Vertical take off position 3^{rd} generation Hopper.

[5] A. Bicchi, A. Balluchi, D. Prattichizzo, and A. Gorelli. Introducing the sphericle: An experimental testbed for research and teaching in nonholonomy. In *IEEE Int. Conf. on Robotics and Automation*, San Diego, CA, May 1997.

[6] J.R. Budenske, M. Dvorak, M. Gini, D.G. Krantz, P.Y. Li, F. Malver, B. Nelson, N. Papanikolopoulos, P.E. Rybski, S.A. Stoeter, R. Voyles, and K.B. Yesin. A miniature robotic system for reconnaissance and surveillance. In *IEEE Int. Conf. on Robotics and Automation*, pages 501–507, San Francisco, CA, Apr 2000.

[7] A. De Luca and G. Oriolo. Stabilization of the acrobot via iterative state steering. In *IEEE Int. Conf. on Robotics and Automation*, pages 3581–3587, Leuven, Belgium, May 1998.

[8] P. Fiorini, S. Hayati, M. Heverly, and J. Gensler. A hopping robot for planetary exploration. In *Proc. of IEEE Aerospace Conference*, Snowmass, CO, March 1999.

[9] J. Hauser and R.M. Murray. Nonlinear controllers for non-integrable systems: the acrobot example. In *American Control Conference*, pages 669–671, 1990.

[10] M.H. Kaplan and H. Seifert. Hopping transporters for lunar exploration. *J. Spacecraft and Rockets*, 6(8):917–922, Aug. 1969.

[11] D.E. Koditschek and M. Bühler. Analysis of a simplified hopping robot. *Int. J. Robotics Reseach*, 10(6):587–605, Dec. 1991.

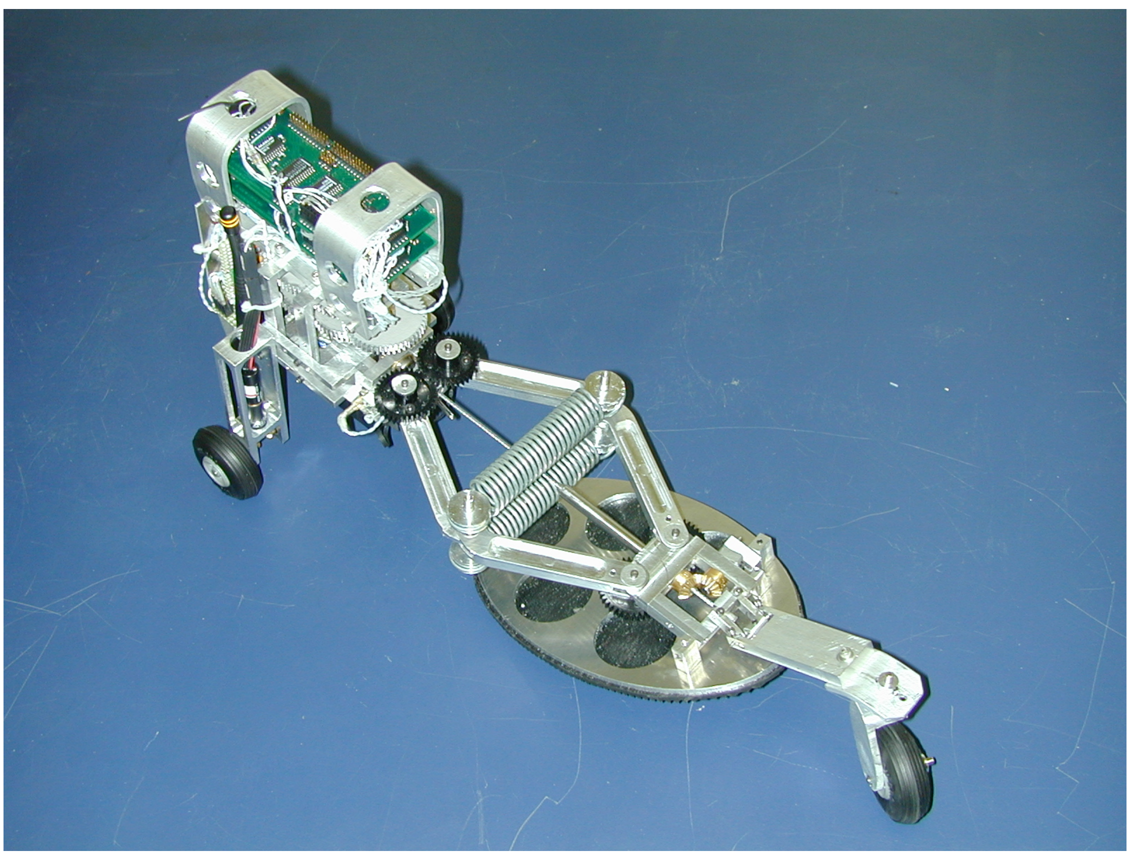

Figure 19: Rear view of the 3^{rd} generation Hopper.

[12] Z. Li and R. Montgomery. Dynamics and optimal control of a legged roboti in flight phase. In *IEEE Int. Conf. on Robotics and Automation*, pages 1816–1821, Cincinnati, OH, May 1990.

[13] L. Lorigo, C. Paul, R. Brooks, J. McLurkin, and M. Moy. Autonomy for Mars exploration. In *Workshop on Planetary Rovers at IROS'97*, Grenoble, FR, September 7-11 1997.

[14] A. Mishkin, J. Morrison, T. Nguyen, H. Stone, and B. Cooper. Operations and autonomy of the mars pathfinder microrover. In *IEEE Aerospace Conf.*, 1998.

[15] J. Oberth. *The Moon Car.* Harper and Brothers, New York, 1959.

[16] Marc H. Raibert. *Legged Robots that Balance.* The MIT Press, Cambridge, MA, 1986.

[17] M'Closkey R.T. and J.W. Burdick. Periodic motion of a hopping robot with vertical and forward motion. *Int. J. Robotics Reseach*, 12(3):197–218, May 1993.

[18] H.S. Seifert. The lunar pogo stick. *Journal of Spacecraft and Rockets*, 4(7):941–943, July 1967.

[19] J.E. Shigley and C.R. Mischke. *Mechanical Engineering Design.* McGraw-Hill, New York, 1989.

[20] M.W. Spong. The swing up control problem for the acrobot. *IEEE Control System Magazine*, pages 49–55, Feb. 1995.

[21] Rich Volpe. Personal communication. Aug. 1999.

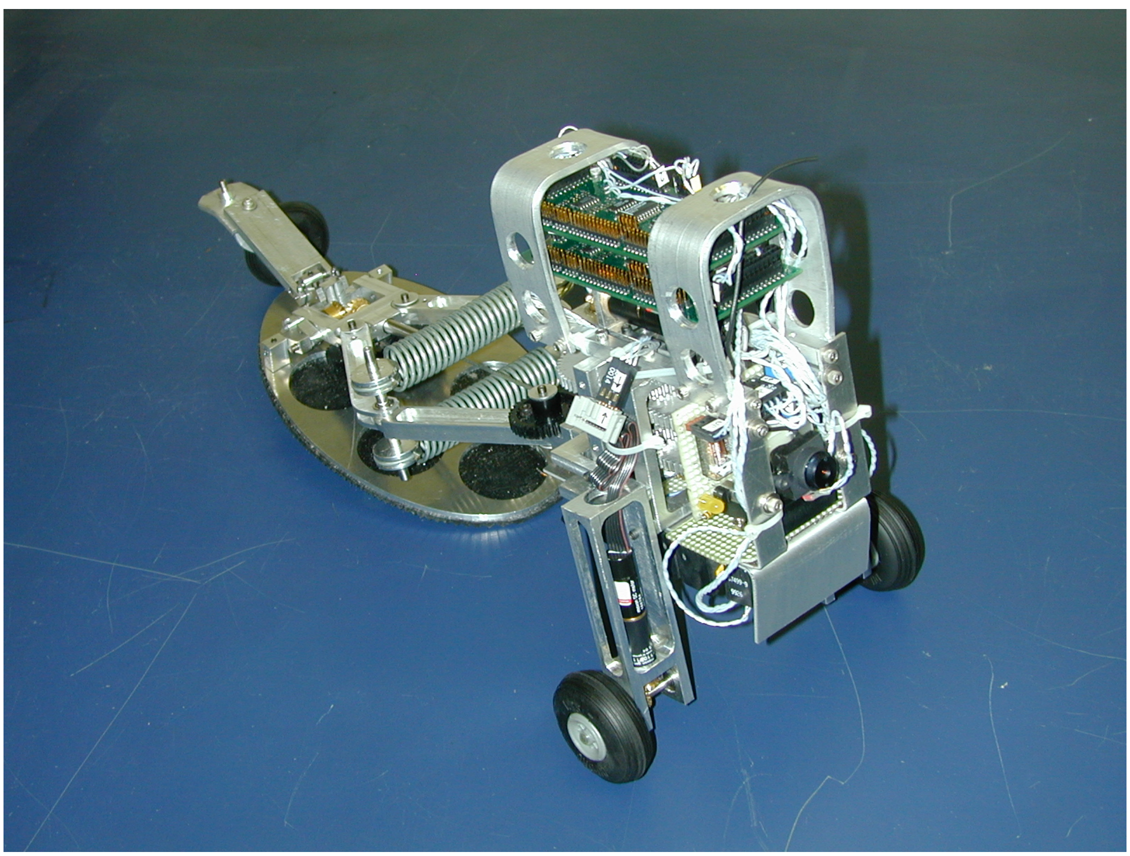

Figure 20: Front view of the 3^{rd} generation Hopper.

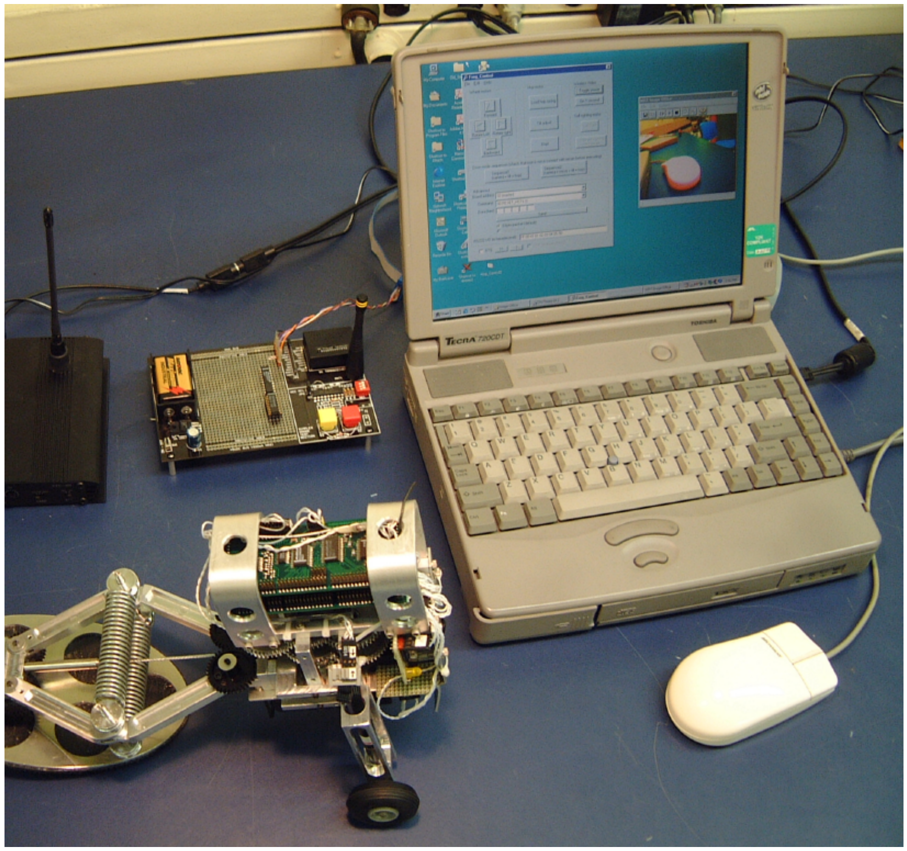

Figure 21: The 3^{rd} generation hopper and its control station.

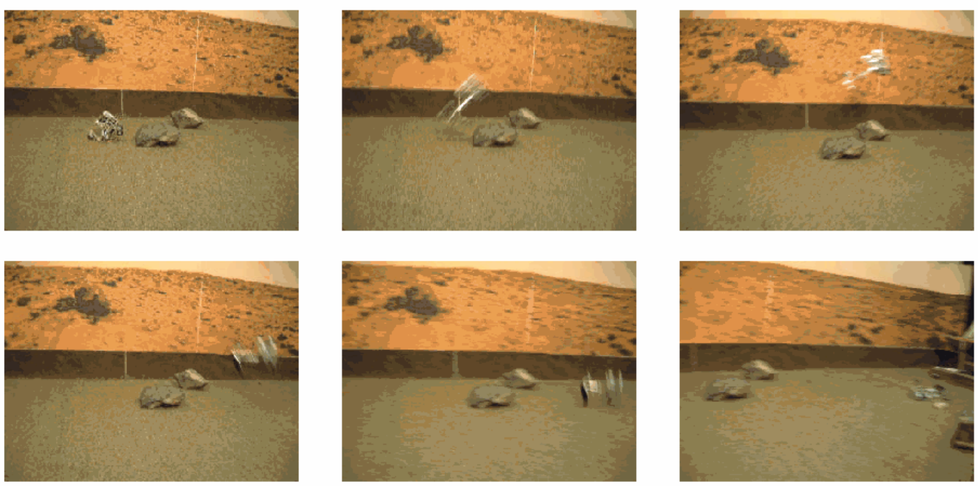

Figure 22: Snapshot of 3^{rd} generation hopper going over a rock

[22] R. Welch, B. Wilcox, and A. Nasif. Nanorover for mars. *Space Technology*, 17(3-4):163–172, April 1998.